

STUDY OF STORM WATER INTAKE STRUCTURE AND ACCUMULATED SOIL REMOVAL SYSTEMS OF DEEP UNDERGROUND LARGE DIAMETER STORM WATER TUNNEL RESERVOIR

大深度・大口径雨水貯留管の取水と堆積物除去に関する実験検討

松田 優*・木村 一政*・佐藤 誠**

Masaru MATSUDA, Kazumasa KIMURA and Makoto SATO

浸水の減少や合流式下水道による河川放流水質の改善を目的として建設される大深度大口径雨水貯留管は、取水時に落下する水の衝撃や流入する土砂の堆積などの問題に配慮して設計する必要がある。そこで雨水貯留管の取水構造と排砂システムに関する研究を行った。研究は、取水構造設計の基礎資料となる水理模型実験と最適な貯留の断面や縦断勾配の設定の基礎資料となる排砂実験の二つの実験を基本に行った。

本論文は1999年8月にオーストラリアで開催された International Conference Urban Storm Drainage に投稿した原稿の再掲である。

Key Words : deep underground large diametric storm water tunnel, flush water volume, inlet, prang pool, sediment discharge, tractive flow discharge, tractive force, vortex-flow drop shaft

1 . PREFACE

In the urban areas of large cities, where there are few plots of vacant land available for public use and highly dense systems of life-supporting facilities are buried under the streets, it is difficult to find space for construction on the land surface or in shallow strata beneath the streets. Therefore, facilities such as sewers, streets and rivers are being buried deeper underground.

The Municipality of Kawasaki City is now building the "Egawa Deep-Underground Large-Diameter Storm Water Tunnel", a storm water reservoir that uses the shield method to reduce the load from overflow during flood mitigation. It also includes a sewer with an inner diameter of 8.5m, a total length of 1,500m and 81,000m³ of water reservoir approximately 35m beneath the surface.

Building a deep-underground large-diameter storm water tunnel involves two main problems(one of them is how to select the water intake structure and design the fall so that falling energy will dissipate itself) since falls become heavy when

storm water is taken in from existing sewers. The other is that it is difficult to collect soil and sand mechanically, because soil and sand coming in from the reserved storm water, which includes organic matter, builds up inside the storm water tunnel along its entire length. It is desirable, therefore, that soil and sand be carried out and removed after they are collected by tractive force and that a system be constructed to remove accumulated soil and sand efficiently. This study deals with these two problems and explains the experimentation design methodology and its results.

2 . STUDY OF WATER INTAKE AND HEAD STRUCTURE

(1) THE STRUCTURE AND PROBLEMS OF A VORTEX-FLOW DROP SHAFT

There are three kinds of water intake and head structure, as shown in Table 1. Since the construction area is small, and the design flow rate and head are too high for the area shown in Table 2, we have decided to adopt a vortex-flow head structure that enables us to reduce the structure for a large quantity of water intake. This structure will be in scale as shown in Figure

* 川崎市建設局 下水道部

** 首都圏事業部 上下水道部

Table 1 Intake and Drop Structure

Intake vertical shaft type		
Vortex-flow	Srep-flow	Helical shoot-flow
Plan		
Profile		

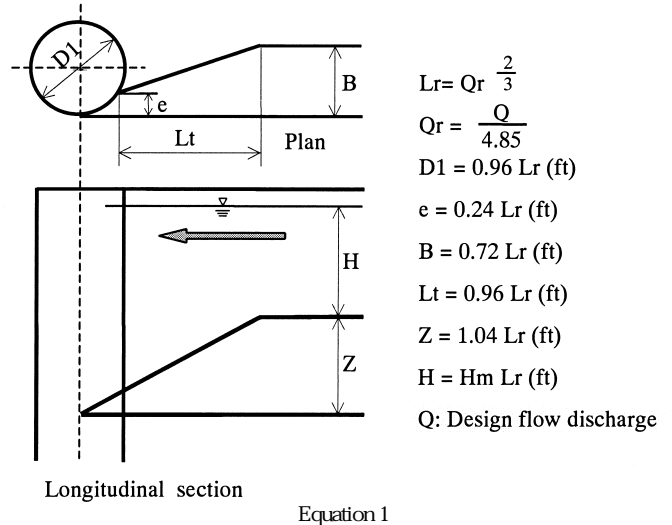


Table 2 Design condition

Item	Volume(m ³ /s)
Design flow discharge	18.048m ³ /sec
Difference of fall	22.7m

1, from the calculation using "Equation 1". In order to design the structure, it is necessary to clarify a) the hydraulic regime from water influx to tunnel reservoir and b) the shock absorption effect and its applied pressure in the absorption tank. Since these could not be clarified theoretically, however, we investigated them using the following hydraulic model experiment.

(2) HYDRAULIC MODEL EXPERIMENT

The hydraulic model of the vortex-flow drop shaft is designed on the flow in an open channel. Therefore, it is important to maintain geometric similarity of the channel, and similarity of the inertial force controlled by gravity. For this purpose, the model shown in Figure 2 was created including the distance of 37 meters between the upper water inflow channel and about 100 meters of the downstream tunnel reservoir in addition to the whole vortex-flow drop shaft. The experiment was conducted in accordance with the measurement method shown in Table 3. The model of the vortex-flow drop shaft used in the experiment was designed on the basis of the specifications obtained from the experiment proposed by Kennedy and Jain (1980).

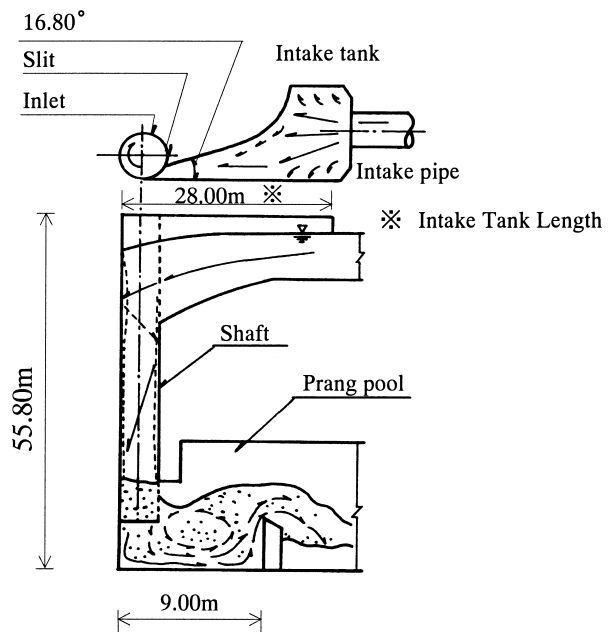


Figure 1 Detail of Vortex-flow Drop

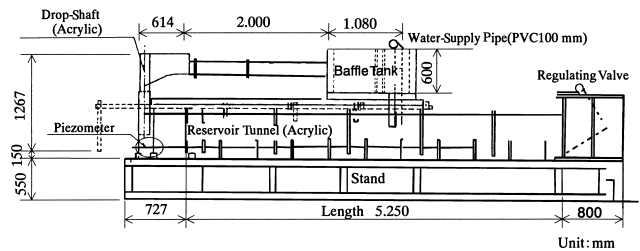


Figure 2 Model

Table 3 Measurement method

Item	Measurement method
Flow discharge	Orifice meter set in water-supply pipe & Manometer for the difference of water pressure
Water level	Point gauge with 1/10 mm reading
Motion velocity	Peter pipe & Electro-magnetic velocity meter & Manometer for water pressure
Water pressure	Measured through the difference of water head in vinyl hose that connect Piezometer & Manometer

(3) RESULTS OF THE MODEL TEST

1) Hydraulic Regime of Influx

As for the hydraulic regime in the inlet tank shown in Figure 3, when flow rate is low (Q=4.512m³/s and Q=9.124m³/s), storm water increases its flow speed immediately after the inlet pipe, runs in supercritical flow, and increases its depth by making

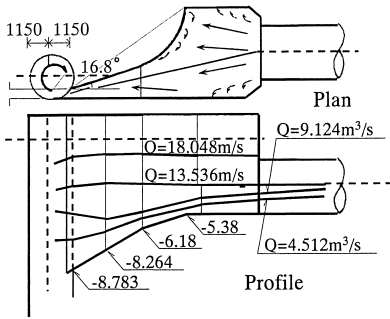


Figure 3 Intake Tank

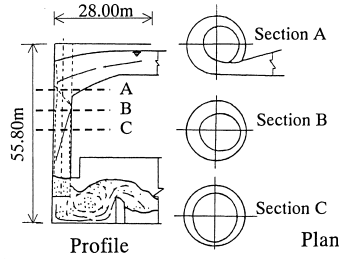


Figure 4 Section of Inlet Tank

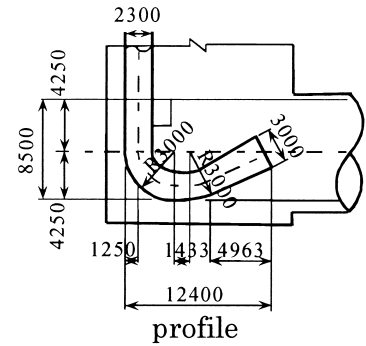


Figure 5 Concept Drawing of Trap

hydraulic jump at the inlet immediately before the influx of the vortex-flow head. The probable reason for this is that the slope of the water channel accelerates the flow to supercritical level at first, following which the reduction in the width of the water channel causes the flow to make a hydraulic jump near the inlet.

If the flow rate is $Q=18.048\text{m}^3/\text{s}$ of design flow rate, supercritical flow is not observed in storm water, and storm water runs towards the inlet in subcritical flow. The hydraulic jump phenomenon, which was observed when a small quantity of storm water flowed, is not observed. The results show that, if a tangential inlet structure is properly designed, the vortex-flow can secure a stable flow-down capacity. Furthermore, the results of the experiment suggest that the shape of the tangential inlet structure will not be adversely affected by backwater on the upper flow of the inlet pipe.

2.) Hydraulic Regime of the Vertical Shaft

The hydraulic regime from the inlet to lower shock absorber, and the air-core of the horizontal section inside the inlet are shown in Figure 4. A water vein that influxes from the slit clings to the wall of the inlet and rolls down by centrifugal force, forming a helical flow. The revolution of this helical flow is very sensitive to inlet speed from the slit and the higher the flow rate, the faster the revolution of the helical flow. Even at a very low flow rate, it forms a helical flow down the wall of the inlet.

The minimum air-core area at the set flow rate takes up approximately 37 % of the shaft cross section in section A. This value is greater than 25 % of the minimum ratio of air-core area stipulated at the flood outlet of the water tunnel at a dam, which, generally speaking, flows at very high rate. It can be judged, therefore, that safety for the downstream is sufficiently secured. Therefore, the shaft diameter of 2,300mm (D) and the slit width (1/4 D) adopted in the experiment can be assumed to be appropriate for the flow-down of the designed flow rate.

3.) Shock Absorption Effect in the Absorption Tank; Operational Pressure

As for shock absorption, experiments were conducted on the plans of the prang pool shown in Figure 1 and the trap shown in Figure 5. In the case of the prang pool plan, a shock absorption effect that is compatible with the tunnel reservoir structure can be attained even if the water inside the tunnel reservoir is not deep enough for the designed flow rate. In the case of the trap plan, however, the scatter condition starts at more than $8.0\text{ m}^3/\text{s}$ of flow rate, and storm water is discharged into the tunnel reservoir without shock absorption. It is feared that this will affect the bottom of the tunnel reservoir at the maximum speed of 15.0 m/s, since a supercritical flow area is generated along the long basin. As a result of these experiments, we have decided to adopt the prang pool plan in our design that minimizes structural effect on the reservoir.

Figure 6 also shows the water pressure at which the base of the lower part of the vertical shaft is affected by the water vein that comes down the vertical shaft. When storm water of the designed flow rate flows in flowhead down, there is a resultant water head of at most 8.5m directly at the bottom of the shaft. This value is approximately 4.0m higher than the 4.5m of static pressure in the center of the prang pool. Since this hydraulic pressure is considered to come from the falling speed, it is estimated that the flow speed that affects the bottom of the prang pool is approximately 9.0m/s. From the study on the hydraulic

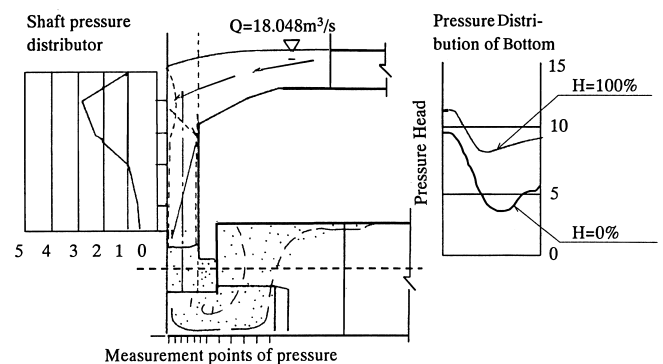


Figure 6 Pressure Distribution

pressure and the progress of abrasion of the concrete due to the high flow speed, we do not think that the concrete will be worn out, judging from the values of the hydraulic pressure and flow speed obtained from the results of the experiment.

(4) DETERMINATION OF WATER INTAKE AND HEAD STRUCTURE

The vortex-flow head has almost never been used in Japan. However, in this case, we believe that it is most suitable as the water intake structure for storm-water tunnel reservoirs because it requires a minimum of space, because it can attain the necessary water conductivity, and because a stable water intake hydraulic regime is secured by it. The structure of the vortex-flow head we have adopted is shown in Figure 1.

3 . GRASPING OF TRACTION CHARACTERISTICS FOR ACCUMULATED SOIL AND GRIT FLUSHING

(1) ACCUMULATION REMOVAL SYSTEM

Storm water reserved in the tunnel reservoir is drained by a pump after the rain stops. The greater part of soil and grit containing organic matter, however, remains inside the tunnel reservoir. In order to prevent the sewage from giving off a bad smell and to keep the inside of the tunnel reservoir in good condition, it is necessary to flush the inner tunnel reservoir. Since the "Egawa Storm-water Tunnel Reservoir," which has an internal diameter of 8.5m and a total length of 1,500m is a gigantic cylindrical shape, it is difficult to remove accumulated soil and grit mechanically. For this purpose, we have decided to

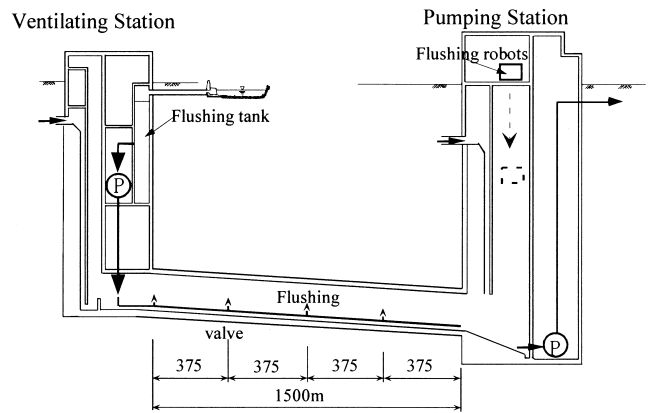


Figure 8 Outline of Flushing System

flush, collect and carry out the accumulated soil and grit with the system shown in Figure 7.

1) Flush water

Flush water will be provided by the flushing tank in the ventilating station shown in Figure 8. We have decided to adopt a flushing tank, the capacity of which is approximately 600m³ due to the restrictions posed by the size of the ventilating station and the condition of the site in this area.

2) Flush

We have decided to adopt a combination of both a flushing pipe and a portable flushing robot in order to remove the extraneous matter at the side of or on the upper surface of the tunnel reservoir, and to carry soil and grit accumulated at the bottom of the tunnel reservoirs all the way to the end. We have also decided to adopt this combination for the bottom of the inside of the tunnel reservoir. This shape includes a sand removal trench at the foot of its circular section, the shape shown in Figure 9, which helps to flush and collect matter effectively with as little water as possible. This was important due to the restricted quantity of flush water. Also, we have

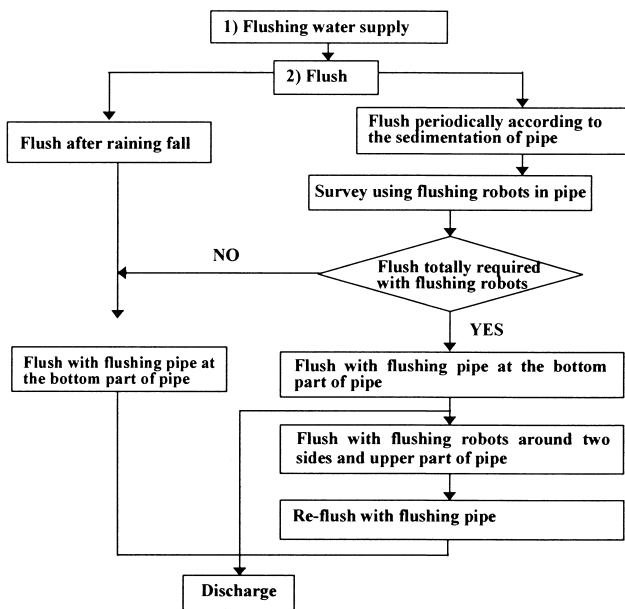


Figure 7 Residue Water-supply System

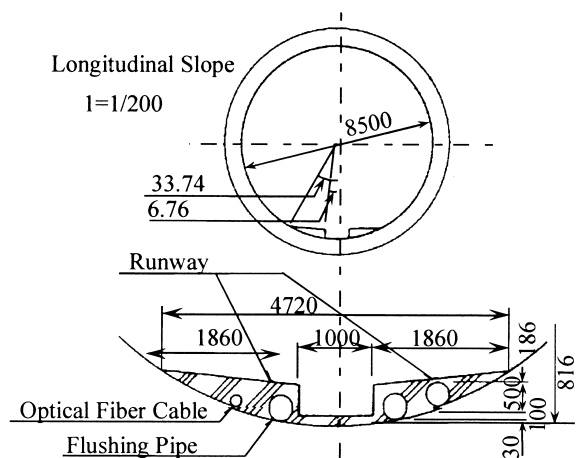


Figure 9 Bottom of Reservoir Tunnel

secured a flat platform measuring approximately 1.8 m-wide in which enough for the flushing robot to run at either side of the platform safely and efficiently, and furthermore for the flushing robot to run. It has also been decided to set the longitudinal slope of the trench at 1/200. This value was decided in consideration of the conditions for building, maintaining and managing a shield tunnel.

3) Flushing pipe

A flushing pipe is a facility for flushing the soil and grit accumulated at the bottom of the pipe down to the end. To be more specific, it is used for conducting flushing water supplied by the flushing tank from an aqueduct buried under the platform on both sides of the trench into the tunnel reservoir, gushing water from a total of four flush valves placed every 375m and washing away the accumulated soil and grit using the current, as shown in Figure 8. The flush point can be selected freely from among the four flush valves.

4) Flushing robots

Flushing robots are used to flush the side or upper part of the inside of the tunnel reservoir which cannot be cleaned by flushing. To be more specific, a robot capable of inspecting and flushing is moved along the sand removal trench and used for inspecting residue inside the pipe, for spraying the flushing water out of the nozzles, for flushing the inside of the pipe and for removing the accumulated soil and grit by water impact. Water is supplied to the robots through the flush valve used for flushing with a flushing pipe.

5) Carrying out Soil and Grit

The soil and grit carried out to the end of the tunnel reservoir in accordance with Flush above are discharged outside the tunnel reservoir by a drainage pump after they are broken into small pieces by the comminuting pump installed at the return pumping station shown in Figure 8.

6) Problems related to the Accumulation Removal System

In practical operation, only the bottom of the tunnel reservoir is flushed using the flushing pipe after each rainfall as already shown in Figure 7. In addition, the inside of the tunnel reservoir is inspected and flushed regularly by the flushing robot. Under this system, however, it is important to clarify traction characteristics for flushing soil and grit accumulated at the bottom of the pipe, but it is difficult to analyze the traction characteristics theoretically. Therefore, we have conducted the following hydraulic model experiments, with the purpose of determining the traction characteristics.

(2) HYDRAULIC MODEL TEST FOR DETERMINING THE TRACTION CHARACTERISTICS

1) Explanation of the Experiments

In the experiments, we observed sedimentation of sand by allowing a fixed amount of sedimentation discharge after piling up sand in the sand removal trench, and also observed the sand removal area (the area in which sand flows out and a waterbed appears) developing in the upper stream. We extracted a 20m-long steel water channel (a partially glassed-in wall) with variable slopes as the experimental water channel as shown in Figure 10. This was used as part of the real sand removal trench, which has a total length of 1,500m and a width of 0.6m. Table 4 shows the comparison between the real sand removal trench and the model.

In the experimental water channel, we used 4m of the upper part as the baffling area, and then covered the downstream distance of 15m with 1-2cm thick sand to prepare for the initial conditions for sand accumulation. Two kinds of sand was used

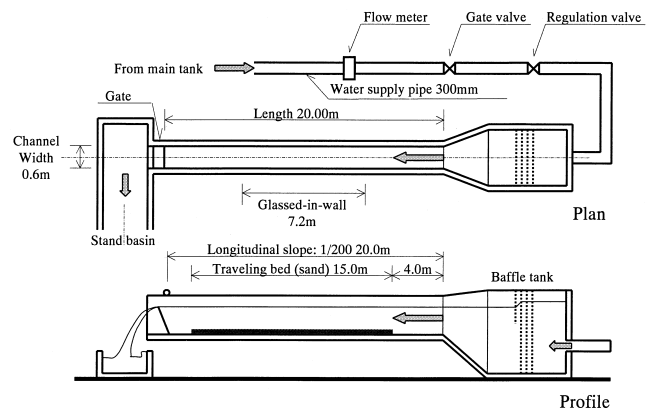


Figure 10 Hydraulic Model Experiment

Table 4 Profile of experiment Sands

Item	Sample sand No.1		Sample sand No.2	
	Model	Prototype	Model	Prototype
Mean particle size of sandy soil d_m (mm)	0.17	0.18	0.71	1.20
Maximum particle size of sandy soil (mm)			5.0	8.3
Uniformity coefficient U	1.6		3.0	
Specific gravity	2.65	2.65	2.65	2.65
Apparent mean accumulated thickness (mm)	20	30	10	20
Real mean accumulated thickness (mm)	8.9	14.8	6.2	10.3

Table 5 Experiment model and real structure

Item	Real structure	Model
Channel width	1.00m	0.60m
Length	33.33m	20.00m
Longitudinal slope	1/200	1/200
Roughness coefficient	0.013	0.012

in the experiment, an almost uniform sand (Sand No.1) with an average grain diameter of 0.17mm, and the other a mixed sand (Sand No.2) with a maximum grain diameter of 5mm and an average grain diameter of 0.71mm. Table 5 shows a conversion of the above into real sand accumulation. All the following figures for sand accumulation conditions show converted to the real structure values.

The experiment was conducted at five flow rates: 0.05, 0.10, 0.20, 0.30, and 0.40m³/s under the fixed flow condition. The water flow experiment was standed by lowering downstream gate after spreading sand and putting up the gate at the end of the area downstream of the water channel. A water depth designated suitable to each flow rate was set by storing water so that the sand would not move. In this case, the flow of the water channel without sand accumulation runs in supercritical flow since the roughness coefficient of sand is n=0.013, while the flow of the water channel with sand accumulation enters subcritical flow as the roughness coefficient increases to n=0.02.

2) Results of the Experiment

a) Moving Configuration of Sand

With a grain diameter of 0.28mm, as shown in Table 6, motion of sand was, generally, in a traction phenomenon at a flow rate of 0.05m³/s and 0.10m³/s. Ripples developed on the bed. When the flow rate exceeded 0.10m/sec., suspended flow developed and the bed became flat. With an average sand grain diameter of 1.2mm, however, the motion of sand was almost in traction up to the flow rate of 0.2m³/s. There was a conspicuous suspended flow of sand when the flow rate exceeded 0.3m³/s. With this sand grain diameter, ripples were not formed on the bed even at on slow flow rate, and the bed was flat.

b) Motion Velocity of Sand

The flushing area of sand that moves from the upper stream takes the shape of a wedge that is wide fat in the center and narrow at both ends as a result of the velocity distribution shown

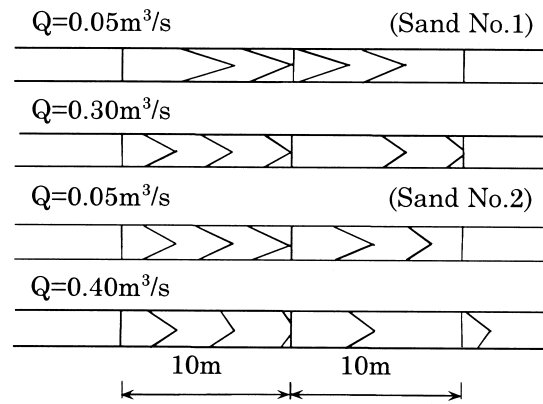


Figure 11 Flushing area of sand

in Figure 11. The slower the flow rate, the sharper the wedge, and the faster the flow rate, the duller the wedge. The top of the accumulated sand area (the boundary between water and sand that are washed away by a current) moves downstream at a more or less constant speed. Almost the same phenomenon occurs even when the sand grain diameter is different. Especially in the case of mixed sand with an average grain diameter of 1.2 mm, the maximum diameter of a grain is approximately 8mm. Yet, in no case did sand of the large diameter remain.

Figure 12 shows the relationship between motion velocity towards the downstream of the top of the accumulated sand area and the flow rate. In an area where the flow rate is comparatively low, the motion velocity increases at an ever-increasing speed in areas in which the flow rate exceeds its criticality (the flow rate that exceeds a critical tractive flow discharge), and its velocity increases in proportion to the flow rate when it is higher than 0.2m³/s. The results show that the smaller in diameter the sand grain, the higher the motion velocity, and that the motion velocity is not inconsistent with an actual physical phenomenon. The above are, however, the experimented results that we obtained by spreading sand

Table 6 Moving configuration of sand

Case	Flow discharge m ³ /s	Bed configuration & motion state	
		Sample sand No.1 (particle size: 0.28 mm)	Sample sand No.2 (particle size: 1.2 mm)
1	0.05	traction state with ripple highly developed	traction state (flat head)
2	0.10	roughly traction state with ripple highly developed	traction state (flat head)
3	0.20	mainly traction state accompanying suspended flow (flat head)	traction state (flat head)
4	0.30	suspended flow developed	accompanying suspended flow (flat head)
5	0.40	apparent suspended flow totally	apparent suspended flow

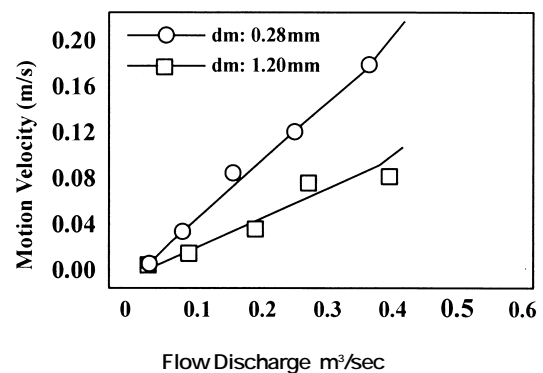


Figure 12 Flow Discharge and Motion

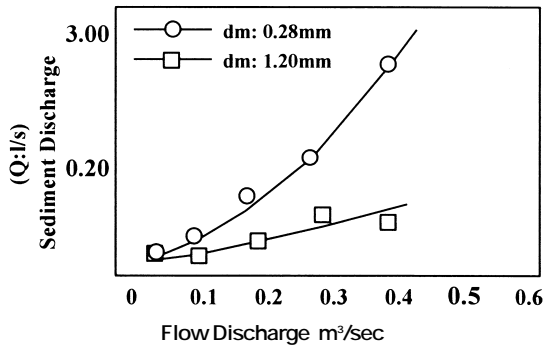


Figure 13 Flow Discharge and Sediment discharge

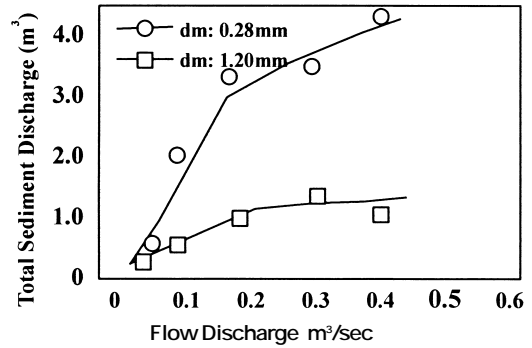


Figure 14 Flow Discharge and Total Sediment Discharge

uniformly over the water channel, and it should be noted that a different phenomenon may be observed when soil and sand are actually spread.

c) Sand Removal Capacity

Figure 13 shows sediment discharge at each flow rate that was obtained from the results of the traction experiments. This sediment discharge was obtained as per unit sediment discharge by multiplying the per unit time motion velocity of the top of accumulated sand area by the accumulation thickness, on the assumption that the top of the accumulated sand area moved at a nearly constant speed and that the accumulation thickness in the accumulated sand area was kept constant. The sediment discharge remains constant in relation to sand grain size, but increases in proportion to the flow rate. However, the absolute volume of the sediment discharge for a grain diameter of 0.28mm is about three times the sediment discharge for a grain diameter of 1.2 mm. From this result, it is possible to estimate sediment discharge in relation to flush water volume.

(3) EFFICIENT DETERMINATION OF FLUSHING FLOW DISCHARGE

Figure 14 shows total sedimentation discharge {= sediment discharge x (600 ÷ flow rate)} at a flushing capacity of accumulated sand and grit with a flush water volume at 600m³. At a given flush water volume, the bigger the unit time flush water volume, the larger the flushing capacity, but the increase in ratio is less pronounced at the border of a per unit time flushing capacity of 0.20m³/s. In the case of the combine particle size of 1.2mm, flushing capacity decreased slightly the flush water volume of 0.4m³/s. This suggests that even if the tractive flow discharge increases, high flush efficiency in proportion to increase in the discharge cannot necessarily be raised, and that total sedimentation discharge cannot be increased according to the increase in the flow rate in excess of a

certain flushing flow discharge. When the relation between the traction capacity and the size of the flush tank facility is considered, it is found that the efficient flush water volume suitable for traction is approximately 0.20 m³/s.

It has been confirmed from the above experiment that the flush water must be 15.3 cm deep in order to flow at on efficient flush water volume of 0.2 m³/sec, if the longitudinal slope is 1/200 in the section of Figure 10, and that adequate safety can be secured at 50cm of the flush water trench depth, which is obtained from the shape of the section for its maintenance.

4 . CONCLUSION

The conclusions we have drawn from the study made mainly on the basis of the hydraulic model experiment are as follows:

- It has been confirmed that the vortex-flow fall construction is suitable as a water intake structure for deep-underground large-diameter storm water.
- It has been confirmed that efficient flushing flow discharge exists in the traction of soil and grit.

The "Egawa Storm-water Tunnel Reservoir" is now being constructed, with a scheduled completion date in the year 2001. We would like to verify a hypothesis of the outcome of this experiment since the Egawa Storm-water Tunnel Reservoir will function as a tunnel reservoir in the near future.

Reference

- 1) AIC Committee 210 (1987), *Erosion of Concrete in Hydraulic Structures*, AIC Materials Journal, March-April, ACI Committee 210, pp. 136-157.
- 2) Iowa Institute of Hydraulic Research (1980). *Vortex-Flow Drop Structures for the Milwaukee Metropolitan Sewerage District Inline Storage System*, IIHR Report No. 264, The University of Iowa, Iowa.
- 3) The American Society for Testing and Materials (1982). *Abrasion-Erosion Resistance of Fiber-Reinforced Concrete*, Cement, Concrete, and Aggregates, pp.3-100